

Effects of thermal and chemical treatments on the structural stability of cellulose acetate nanofibers

Yaser E. Greish^{a,*}, Mohammed A. Meetani^a, Eisa A. Al Matroushi^b, Bothaina Al Shamsi^c

^a Department of Chemistry, College of Science, United Arab Emirates University, P.O. Box 17551, Al Ain, United Arab Emirates

^b Department of Chemical and Petroleum Engineering, College of Engineering, United Arab Emirates University, P.O. Box 17551, Al Ain, United Arab Emirates

^c Al Ain Municipality, P.O. Box 25000, Al Ain, United Arab Emirates

ARTICLE INFO

Article history:

Received 30 March 2010

Received in revised form 8 May 2010

Accepted 11 May 2010

Available online 19 May 2010

Keywords:

Cellulose

Nanofibers

Thermal stability

Alkali treatment

Microstructure

ABSTRACT

Cellulose nanofibrous membranes made by electrospinning are characterized by their high porosity and interconnectivity, and therefore, considered potential candidates for ultrafiltration processes. Due to the difficulty to dissolve cellulose, electrospinning of cellulose derivatives followed by regeneration of cellulose is a more convenient approach. Using a previously optimized set of electrospinning parameters, the effects of thermal and chemical treatment of cellulose acetate (CA) nanofibers on their structural stabilities are thoroughly discussed in the current article. Nanofibrous membranes initially made from solutions containing 10–20 wt% CA were investigated. Structural stability was monitored using infrared spectroscopy (IR), differential scanning calorimetry (DSC), and scanning electron microscopy (SEM) techniques. Results showed the possibility of de-acetylation of CA nanofibers during the thermal treatment step, more precisely on the procedure and temperature of treatment. Combining thermal and alkali treatment of CA nanofibers was found crucial to their morphologies. Optimization of these processes is, therefore, attempted. Phase purity of the regenerated cellulose nanofibers was investigated.

© 2010 Elsevier Ltd. All rights reserved.

1. Introduction

Natural cellulose fibers normally have dimensions within the micrometer scale. Recently, the formation of cellulose nanofibers has attracted a great deal of attention due to their good thermal stability, chemical resistance, biodegradability, and others (Kaur, Ma, Chan, Ramakrishna, & Matsuura, 2006). These properties have resulted in a wide range of applications in affinity membranes, biosensors, chemosensors, protective cloths, reinforced nanocomposites, and others (Kaur et al., 2006). Among the different methods of making cellulose nanofibers, an electrospinning has been widely used. This technique is based on the application of a high voltage on a polymeric solution with an appropriate viscosity (Zeleny, 1914). If the applied voltage overcomes the surface tension of polymer droplet, the later elongates as it exits a spinneret and deposits on a grounded collector in the form of nanofibers (Zeleny, 1914). These nanofibers could be made uni-directionally aligned or non-woven. A non-woven network of polymeric nanofibers is characterized by the presence of highly interconnected pores, which make these

membranes viable for filtration industry (Barhate & Ramakrishna, 2007).

Electrospinning of cellulose is not an easy process because of its weak solubility in traditional solvents (Kim, Kim, Kang, Marquez, & Joo, 2006; Xu et al., 2008). Solvents such as N-methyl-morpholine N-oxide/water (NMMO/water), lithium chloride/dimethylacetamide (LiCl/DMAc) and other ionic liquids have been recently used to fabricate electrospun cellulose nanofibers (Han, Son, Youk, & Park, 2008; Han, Youk, Min, Kang, & Park, 2008; Kim, Frey, Marquez, & Joo, 2005; Kim et al., 2006; Kulpinski, 2005; Xu et al., 2008; Zhang, Menkhaus, & Fong, 2008). However, these solvents cannot completely evaporate during the electrospinning process, while removal of lithium or chlorine ions from the electrospun fibers was very difficult (Frey, 2008). On the other hand, cellulose nanofibers were made by high temperature electrospinning of cellulose melts (Kim, Chen, Kang, Park, & Schwartz, 2008). Thicker fibers with diameters up to 1000 nm were obtained. To enhance the solubility of cellulose and hence its electrospinnability, cellulose derivatives have been extensively exploited (Frenot, Henriksson, & Walkenstrom, 2007; S.O. Han et al., 2008; Han, Son, Youk, Lee, & Park, 2005; S. Han et al., 2008; Liu & Hsieh, 2003; Park, Han, & Lee, 2007; Son, Youk, Lee, & Park, 2004; Tungprapa et al., 2007; Wang, Wang, & Huang, 2007; Wu, Wang, Yu, & Huang, 2005; Zhao, Wu, Wang, & Huang, 2003; Zhao, Wu, Wang,

* Corresponding author. Permanent address: Department of Ceramics, National Research Center, Cairo, Egypt. Contact information in UAE: Tel.: +971 50 233 8203; fax: +971 3 767 1291.

E-mail address: y.afi@uaeu.ac.ae (Y.E. Greish).

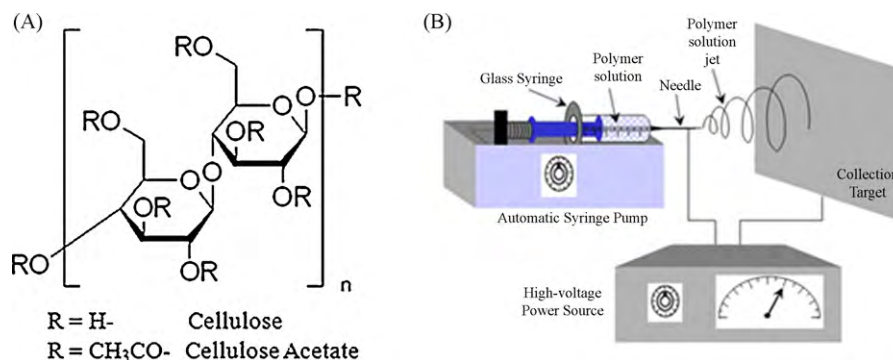


Fig. 1. Schematic diagram of (A) the electrospinning setup, and (B) chemical structure of cellulose and cellulose acetate.

& Huang, 2004). Among these derivatives, cellulose acetate was used in different solvent systems to produce nanofibers that were then converted to cellulose by de-acetylation (Chen, Bromberg, Hatton, & Rutledge, 2008; Liu & Hsieh, 2002; Lu & Hsieh, 2009; Ma & Ramakrishna, 2008; Ritcharoen, Supphol, & Pavdsnt, 2008; Yoon, Moon, Lyoo, Lee, & Park, 2009; Zhao et al., 2003). Investigators concluded that a proper solvent system for cellulose acetate should be a mixture of polar and non-polar solvents. Rheology and homogeneity of the obtained solutions using each solvent dictated the produced nanofibers' characteristics. It was found that stand-alone solvents were not useful in obtaining homogeneous nanofibers. Instead beads were formed within the nanofibrous membranes obtained (Zhao et al., 2003). In a previous article, we have successfully optimized the conditions of electrospinning of cellulose acetate in an acetone/dimethyl acetamide solvent system (Al Shamsi, 2009). In order to re-generate cellulose, chemical treatment of CA nanofibers in alkaline solutions was suggested. Before, doing that, researchers have recommended the thermal treatment of the as-spun CA nanofibers to maintain the mechanical integrity of the formed CA nanofibers. Thermal treatment is carried out at temperatures above the glass transition temperatures of CA and below their melting points. Ma et al. thermally treated CA sheets sandwiched between Teflon plates at 208–210 °C for 1 h, followed by treatment in 0.1 M NaOH solution in water/ethanol for 24 h at room temperature (Ma, Kotaki, & Ramakrishna, 2005). Son et al. carried out the same process in 0.5 N ethanolic solution of KOH for 24 h after swelling the as-spun CA nanofibers in acetone/water (1:1) solutions for 24 h (Son et al., 2004). Han et al. conducted this process on the as-spun CA nanofibers in both aqueous and ethanolic solutions of KOH (0.5 N in each) for 3 h and observed swelling of those fibers treated in aqueous media compared to those treated in ethanolic media (S.O. Han et al., 2008; S. Han et al., 2008). Using a more diluted ethanolic solution of 0.05 M NaOH, Zhang et al. (2008), Lu and Hsieh (2009), and Tang and Liu (2008) conducted this process in 24 h on the as-spun CA nanofibers. Liu and Hsieh (2002) conducted the same process, also on as-spun nanofibers, in 0.05 N NaOH aqueous and ethanolic solutions for up to 140 and 60 min in aqueous and ethanolic solutions, respectively. The current article investigates the effect of thermal treatment of CA nanofibrous membranes at temperatures up to 208 °C in different conditions, followed by detailed quantification of the de-acetylation of CA to regenerate cellulose nanofibers in alkaline media. De-acetylation of the as-spun non-thermally treated nanofibers was also carried out.

2. Experimental work

Cellulose acetate (CA) used in the current study was obtained from Sigma–Aldrich, USA, with a 39.7 wt% acetyl content and an

average M_n ca. of 50,000 (by gel permeation chromatography; GPC; Fig. 1A). As a reference material, cellulose in the form of micro-crystalline powder with an average particle size of 20 μm was used. Solvent system used to dissolve CA included N,N-dimethyl acetamide (DMAc); obtained as a ReagentPlus[®] with a min. assay of $\geq 99\%$, and acetone; that was purchased from Merck, Darmstadt, Germany with a min assay of $\geq 99.8\%$. Ethyl alcohol and tetrahydrofuran were also obtained from Sigma–Aldrich, USA as analytical reagents with a min assay of 96%. Sodium hydroxide was also obtained from Sigma–Aldrich, USA in a powder form as A.C.S. reagents of 99+% min assay. A solvent mixture containing acetone and DMAc, at a volume ratio of 2:1, was prepared by stirring their respective volumes at room temperature for 1 h. Solutions containing 10, 12, 15, 17 and 20% of CA, as weight of CA per volume of the solvent mixture, were prepared by dissolving the appropriate amount of CA powder in the solvent mixture with warming at a temperature around 30–35 °C. Solutions were kept in their beakers, completely sealed by a parafilm and aluminum foil to avoid evaporation of the solvents, until being used in electrospinning.

Parameters affecting the morphology and fiber size distribution of the obtained nanofibrous membranes were previously optimized (Greish et al., unpublished work). In brief, a high voltage power supply, Gamma High Voltage Research, FL, USA, operating at 12 kV was used. All polymer solutions were electrospun onto a grounded collector covered by an aluminum foil, vibrating at 100 rpm, in a home-made plexiglass chamber that was pre-saturated with acetone for 30 min. Pre-optimized electrospinning conditions utilized with all CA solutions included a flow rate of 4 mL/h, and a needle tip-to-collector distance of 14 cm. At the end of every experiment, the fibrous membranes collected on the Al foil was kept in the fuming hood at room temperature for 24 h, to evaporate the remaining solvents. Each membrane was further dried at 100 °C for another 24 h to ensure the removal of all trapped solvents. In order to study the effect of applying a high voltage on the structural integrity of cellulose acetate, phase purity, molecular weight, and thermal characteristics of the prepared nanofibrous media were investigated by infrared spectroscopy (IR), gel-permeation chromatography (GPC), and differential scanning calorimetry (DSC) techniques, respectively, and were compared to those of the as-received CA material. Phase composition and molecular weight of a representative electrospun CA sample were determined and compared to those of the as-received CA polymer, using IR and GPC techniques, respectively. IR characterization was carried out using a Nicolet Nexus 470 IR spectrophotometer, USA. All samples, pre-pressed with KBr, were scanned over the normal range of 4000–400 cm^{-1} using a reflectance mode. GPC was carried out using an Agilent HP 1200 apparatus, Santa Clara, USA, connected to HPchem data acquisi-

tion system. An Agilent PLgel mixed-C separation column; 300 mm length, 7.5 internal diameter, and 5 μm packing particle size operating at a temperature of 25 °C, was used in this regard. THF was used as a mobile phase at a flow rate 1.0 mL/min isocratic elution was used over 15 min. Injection volume was 20 μL . Detection was obtained using refractive index detector and a UV detector at a wavelength 254 nm. The GPC was pre-calibrated with 12 narrow molecular weight distribution polystyrene standards over the molecular weight range of 162 g/mol to 5.0×10^6 g/mol. Thermal characteristics of the electrospun CA nanofibers were also investigated and compared to the as-received CA polymer. Together with IR and GPC techniques, thermal characteristics further confirm the structural integrity and stability of the electrospun CA nanofibers. A differential scanning calorimeter (DSC 200F3-NETZSCH), Germany, was used. Based on preliminary experiments, samples were heated in air at a rate of 20 °C/min for a maximum temperature of 270 °C, which is slightly higher than the melting temperature of CA (Liu & Hsieh, 2002; Meier, Kanis, & Soldi, 2004).

Thermal treatment of the nanofibrous media was carried out at temperatures of 100, 150, and 200 °C in an oven. Selected CA membranes, 9 cm² surface area/each, were placed between 2 Teflon sheets, 100 cm² in surface area and 3 mm in thickness/each. Each assembly was heated for 1 h at the previously mentioned temperatures. In a parallel experiment, selected CA membranes were placed in open Pyrex beakers and heated at the same temperatures for the same time periods. At the end of each thermal treatment, the heated membranes were taken to room temperature, and then analyzed for their structure and morphology using IR and scanning electron microscopy (SEM), respectively. Morphologies of the nanofibrous membranes were assessed using a Quanta inspect scanning electron microscope, The Netherlands, operating at a maximum voltage of 20 kV. Uncoated samples morphologies were collected at both low and high vacuum modes; depending on the samples surfaces features and charging problems faced during the SEM sessions.

The effects of treatment of CA nanofibrous membranes with alkaline solutions on the composition, thermal characteristics and morphology of these media were studied. As spun-CA membranes were first weighed, on dry basis, then soaked in acetone/de-ionized water (1:1 by volume) mixtures for 24 h. Exactly 10 cc of a 0.5 M solution of NaOH was added to each membrane soaked in the acetone–water solutions. Membranes were removed from these alkaline solutions after 5, 10, 15, 20 and 24 h, rinsed with fresh de-ionized water for more than five times, then dried until a constant weight. Each of the post-treatment alkaline solutions was titrated against 0.5 M HCl solution to determine the exact volume of NaOH used in the de-acetylation of CA nanofibrous membranes. Completely dry CA membranes were then examined for their composition and morphology by IR and SEM techniques, respectively. A representative CA sample, that was thermally treated at 208 °C for 1 h, was also subjected to further treatment in an alkaline solution for 24 h. Its phase composition and morphology were also investigated.

3. Results and discussion

3.1. Characteristics of optimally prepared cellulose acetate nanofibers

In a previous article, the different parameters governing the electrospinning of CA were optimized. Those were CA concentration in the acetone–DMAc solvent mixture, the applied operating voltage, the flow rate, and the spinning distance. It was also shown that pre-saturating the electrospinning chamber with ace-

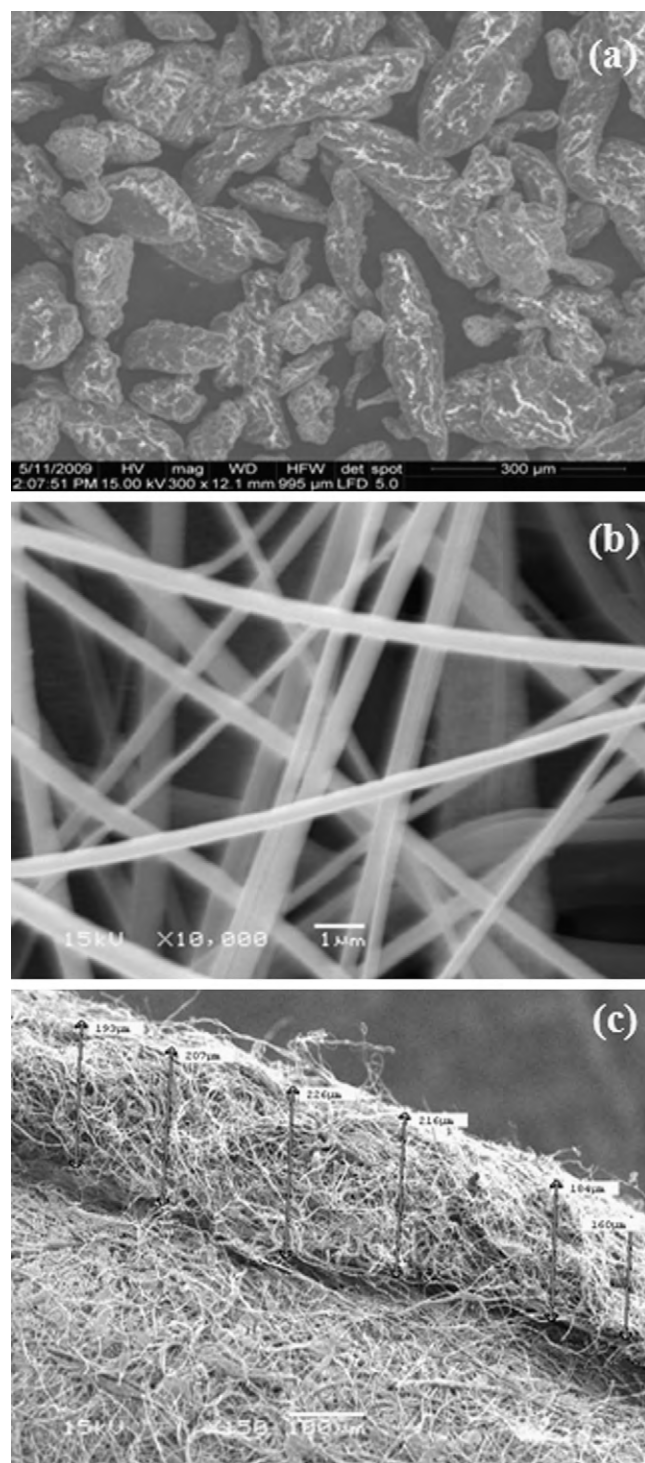


Fig. 2. Scanning electron micrographs of (A) as-received CA powder, (B) electrospun cellulose acetate nanofibers, and (C) a cross section of an electrospun cellulose acetate membrane showing its thickness.

tone and using a vibrating grounded collector have also helped fine tune the characteristics of the produced fibers. The main criteria that were used to optimize the electrospinning parameters was the fiber morphology; its diameter and smoothness, as well as the homogeneity of the fiber and pore size distribution within a nanofibrous membrane. Fig. 2A and B shows the morphology of as-received CA powder compared to as-electrospun CA sample. It is shown that irregular shaped CA particles were converted

to fine homogeneous nanofibers with an average fiber diameter of 380 nm, together with a uniform pore size distribution. Fig. 2C illustrates a cross section of a typical nanofibrous membrane prepared at the previously optimized conditions, showing that an average thickness of a nanofibrous membrane of 150 nm could be achieved. The randomness of the fibers distribution is a main characteristic of fibers made by electrospinning (Taylor, 1964). This results in an interlocking between the fibers, creating interconnected porosities with different dimensions. Despite its random depositions, the overall distribution of the fibers is still homogeneous, and is thus expected to result in a homogeneous pore size distribution as well. It should be mentioned that thicker membranes could be prepared at the optimized conditions if more volume of the polymer solution was injected through the spinneret.

The structural stability of the electrospun fibers was maintained during the electrospinning process. This was confirmed by comparing the infrared spectra of the as-received CA to the as-spun CA sample; Fig. 3A. Both spectra showed the characteristic bands of CA, especially the presence of both –OH and –C=O characteristic stretching bands at 3600–3200, and 1760 cm^{-1} , respectively (Barud et al., 2008). These bands confirm the partial substitution of –OH groups along the cellulose structure by the acetyl groups, where CA is known to contain 39.7 wt% acetyl content. However, the uniformity of substitution, and the presence of this percentage of acetate groups in the structure of CA could not be confirmed by IR. The effect of applying electrostatic forces on the structural

stability of CA during its spinning into nanofibers was also studied by following up the changes, if any, in the molecular weight of CA after spinning. Fig. 3B shows GPC spectra of as electrospun CA fibrous sample from a solution containing 17 wt% of CA. Molecular weight analysis obtained using the UV and refractive index detectors revealed the same M_n value of 46,000 for the as spun sample, which is the same as what was previously measured for the as-received sample. Both IR and GPC results indicated that electrospinning did not affect the structural characteristics of the polymer nor did reflect signs of degradation as a result of the high voltage imposed on the polymer.

3.2. Effect of thermal treatment on cellulose acetate nanofibers

Fig. 3C shows the DSC spectra of the as-spun versus the as-received CA samples, both heated up to 270 °C. The glass transition (T_g) and melting (T_m) temperatures of CA are known to be around 198–205 °C and 224–230 °C, respectively (Liu & Hsieh, 2002; Meier et al., 2004). The glass transition temperature of the as-received CA was calculated to be around 180 °C. Fig. 3C show two endotherms with peak temperatures of 107.2 and 236.1 °C, respectively in the graph of the as-received CA sample. The first broad endotherm is attributed to the evolution of water vapor, which is strongly adsorbed on the CA powder by hydrogen-bonding. The second endotherm may be attributed to T_m of CA. Thermal results of CA thus confirm its structure. Thermal treatment of CA nanofibers

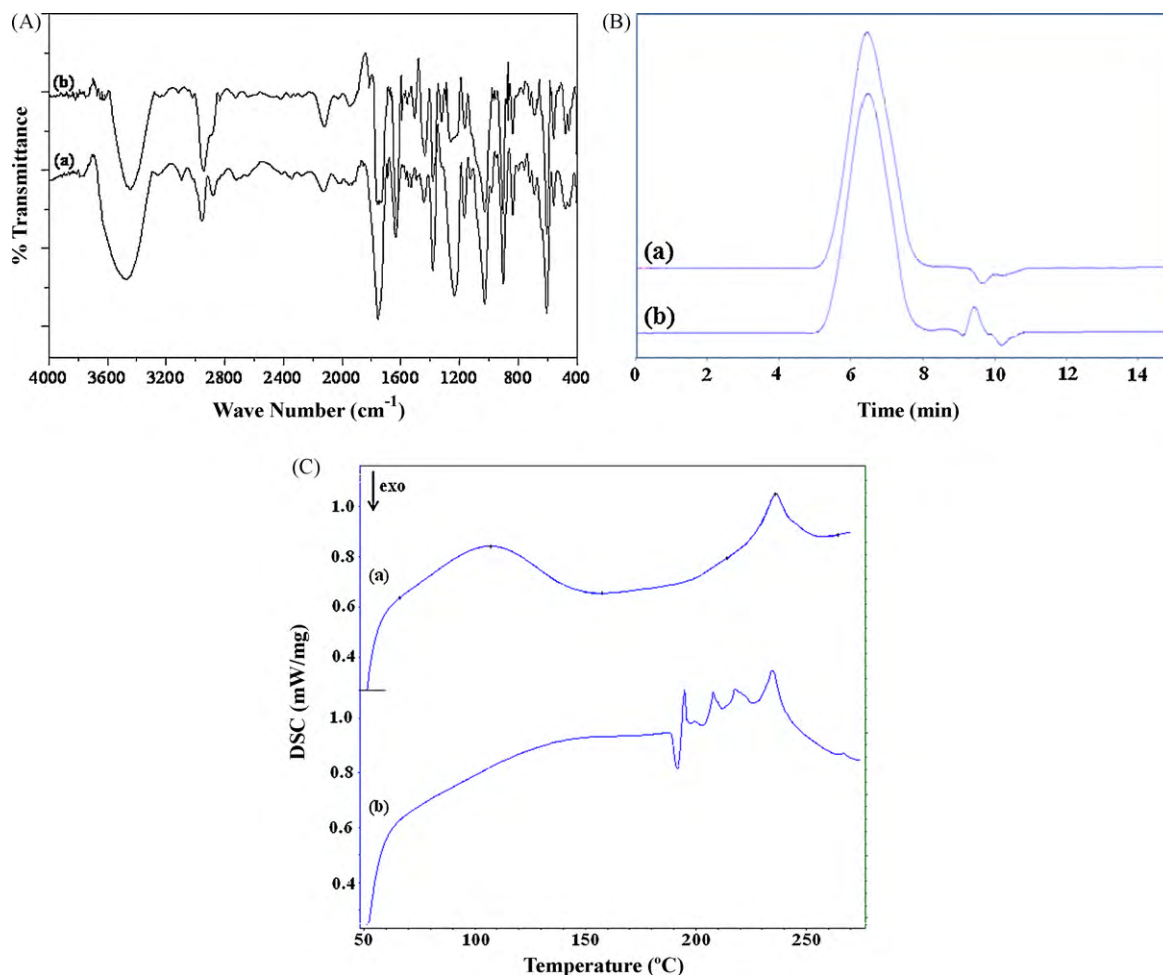


Fig. 3. (A) Infrared spectra of (a) as-received and (b) as electrospun cellulose acetate. (B) Gel permeation chromatographic diagrams of (a) as-received and (b) as electrospun cellulose acetate. (C) Differential scanning calorimetric curves of (a) as-received and (b) as electrospun cellulose acetate.

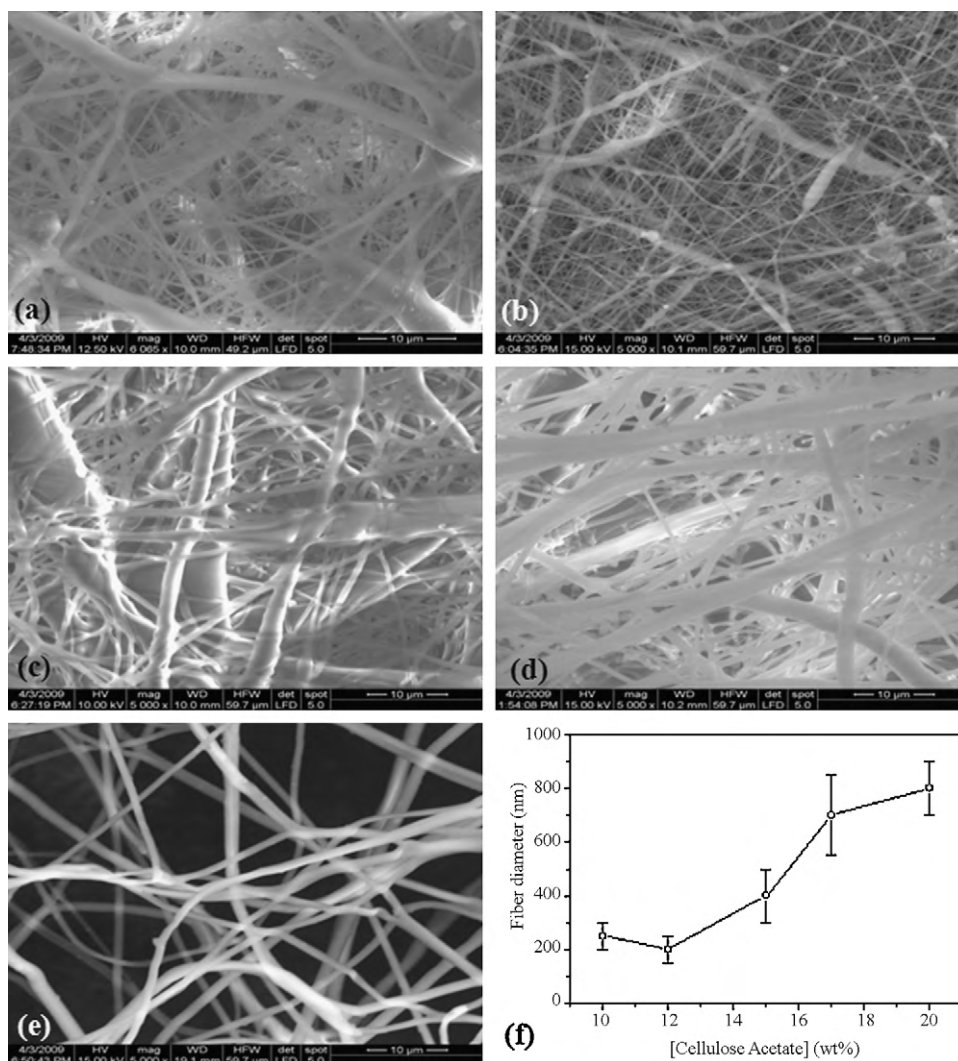


Fig. 4. Scanning electron micrographs of nanofibers electrospun from solutions containing (A) 10 wt%, (B) 12 wt%, (C) 15 wt%, (D) 17 wt%, and (E) 20 wt% cellulose acetate after thermal treatment in air at 208 °C for 1 h, (F) average fiber size distribution as a function of distance.

was previously recommended in order to confirm the removal of remaining solvents and improve the mechanical integrity of the membranes (Ma et al., 2005). The current results suggest a temperature range for thermal treatment of CA to be within a range of >180 to <236 °C to avoid degradation of CA. DSC of the as-electrospun CA membrane; shown in Fig. 3C, indicates the absence of the dehydration endotherm. This is attributed to the evolution of all water of hydration as a result of drying these membranes at 100 °C for 24 h before carrying out its DSC testing. A couple of endotherms were observed between 190 and 235 °C. The last endotherm, at 230 °C, is attributed to the melting temperature (T_m) of CA nanofibers, which is in accordance with that observed for as-received CA. The three endotherms at 190, 208 and 215 °C are, therefore, attributed to a series of events taking place at these temperatures before melting of the fibers, as will be shown later in the current manuscript. A glass transition temperature (T_g) of around 186 °C was calculated for the as-electrospun CA sample, which is slightly higher than that of the as-received CA shown in Fig. 3C. A final conclusion in this respect is the absence of any thermal events at temperatures below 186 °C, indicating its expected stability up to this temperature. In fact, at temperatures below the melting temperature of CA, the chemical structure stability of CA is presumably constant.

Based on the above findings, a temperature of 208 °C was selected to thermally treat the nanofibrous membranes electrospun from solutions containing various concentrations of CA. Previous studies have shown that this temperature was optimum to strengthen the fibers and confirm the removal of any remaining solvents. The micrographs in Fig. 4 ensure the complete removal of solvents. However, a gradual increase in the fiber diameter was also observed with increasing the CA concentration; Fig. 4F. The least average fiber diameter of 200 nm was achieved in those thermally treated membranes spun from solutions containing 12 wt% of CA. There was no indication from the micrographs of these thermally treated membranes of structural deformation of the fibers as a result of thermal treatment. Fig. 5 shows the IR spectra of these membranes. The IR spectra of CA 10 and 12 illustrate the thermal stability of the CA fibers as indicated by their similarity to that of as received and as spun CA samples shown in Fig. 3A. The IR spectra of CA 15, 17 and 20, however, reflected the absence of the C=O group that is characteristic to the acetyl group around 1750 cm^{-1} . This indicates the de-acetylation of the CA fibers and the formation of cellulose fibers instead, reflecting the instability of membranes made of these concentrations in particular to thermal treatment at 208 °C. Visually, these later sheets showed brownish yellow color after thermal treatment, compared to a stable

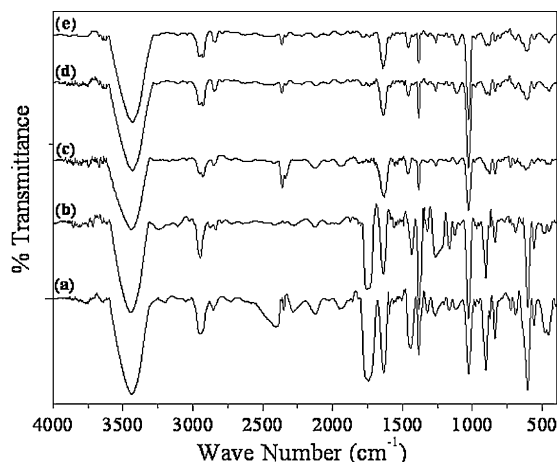


Fig. 5. Infrared spectra of nanofibers electrospun from solutions containing (a) 10 wt%, (b) 12 wt%, (c) 15 wt%, (d) 17 wt% and (e) 20 wt% cellulose acetate after thermal treatment in air at 208 °C for 1 h.

white color of the CA 10 and 12 membranes. Despite this coloration of the sheets, their mechanical integrity was not affected. A closer investigation of all samples indicated that those thermally affected sheets were originally thinner (around 100 μm) than the CA 10 and 12 membranes (around 150 μm). It should be mentioned that each membrane was originally sandwiched between 3 mm Teflon sheets to avoid direct exposure of the sheets to heat (Ma et al., 2005). The thermal instability is, therefore, attributed to a local concentration of heat on these thin sheets, resulting in their instability. To confirm these findings, a CA 12 membrane, with a thickness of around 100 μm , was cut to four equal sections. These were thermally treated at 150 and 200 °C for 1 h at each temperature. Two samples were similarly sandwiched between Teflon sheets, while the two other samples were kept in a Pyrex beaker at these temperatures. Fig. 6 shows IR spectra of the four samples. These spectra show the disappearance of the acetyl carbonyl (C=O) group at 150 and 200 °C in samples sandwiched between Teflon sheets. On the other hand, those samples treated in an open Pyrex beaker showed an initial decrease in the intensity of the acetyl carbonyl group at 150 °C compared to that of the as-spun spectrum. This band showed a further decrease in intensity by raising the temperature to 200 °C. These results are therefore in agreement with those obtained for the CA 15, 17, and 20 samples previously shown in Fig. 5. These findings indicate that what was known as thermal stability of CA up to 208 °C (Ma et al., 2005), was most probably of thick samples (>100 μm thickness). Careful investigation of the IR outcomes, therefore, leads to an explanation of the thermal events previously shown as endotherms at 190, 208 and 215 °C in the DSC spectrum of CA nanofibers; Fig. 3C. It can be concluded at this point that the removal of the acetate group from the CA nanofibers starts at temperatures right below 190 °C, especially in thin membranes and/or small CA nanofibers, where both are characterized by high surface area, which can be considered a strong parameter that enhanced the thermal de-acetylation process.

3.3. Effect of alkali treatment on cellulose acetate nanofibers

Treatment of cellulose acetate in alkaline solutions is known to result in the removal of the acetate groups and the regeneration of cellulose (Son et al., 2004). Therefore, the objective of this step was to investigate its effect on the integrity and morphology of the regenerated cellulosic fibrous membranes. As was discussed above, thermal treatment was found to result in the partial removal of the

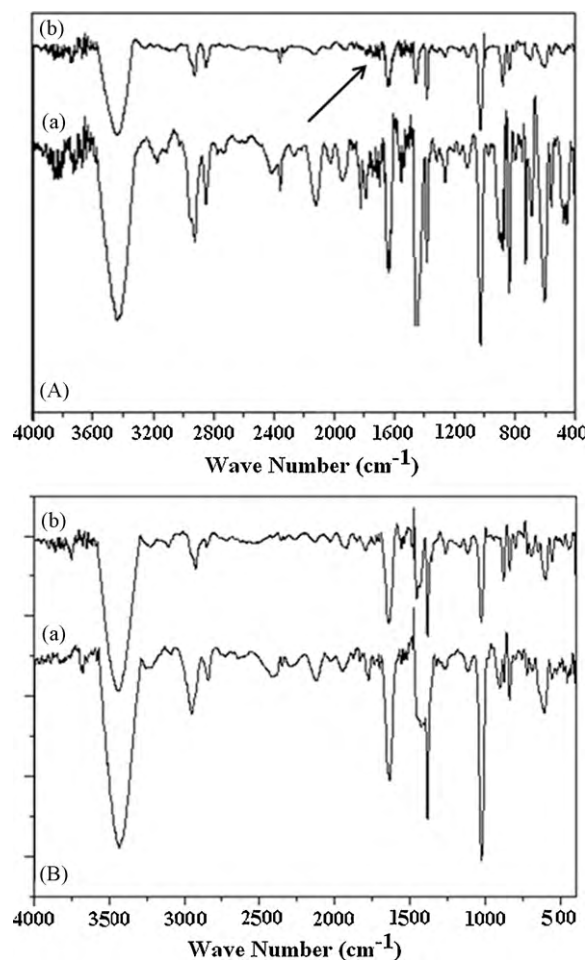


Fig. 6. Infrared spectra of cellulose acetate nanofibrous membranes electrospun from solutions containing 12 wt% of cellulose acetate and thermally treated at (a) 150 °C and (b) 200 °C while (A) sandwiched between 4 mm thick Teflon sheets and (B) left in pyrex beakers.

acetate group from the CA chains. Therefore, the first experiment in this regard was to confirm the removal of this group from a thermally treated membrane in which traces of acetate group was still observed in its IR spectrum. Fig. 7A shows a SEM micrograph of a CA 12 membrane, 100 μm thickness, that was sandwiched between Teflon sheets, thermally treated at 208 °C followed by soaking in 0.5 M NaOH solution for 24 h, then completely dried at 100 °C for 24 h. Distortion of the fibers morphology is the main observation that can be implied from the micrograph. This is expected to highly influence the mechanical integrity of the treated membranes. On the other hand, this was not found to affect the chemical composition of the membranes where its IR spectrum revealed the presence of cellulose as the only phase; Fig. 7B. These findings indicate that regeneration of cellulose from thermally treated membranes may take place completely but on the expense of the quality of the fibers morphology. To avoid these circumstances and to fabricate undeformed high quality cellulose fibrous membranes, regeneration of cellulose was decided to be carried out on fibrous membranes that were only dried at 100 °C without further thermal treatment. As a result of the alkali treatment, the volume of un-reacted NaOH was determined by titrating the remaining NaOH against a standard 0.5 M HCl solution. Fig. 8A shows the volumes of HCl needed to neutralize the un-reacted NaOH in each of the alkaline solutions after each time period of soaking the different membranes in them. All samples showed a decrease in the volume of HCl needed to neutral-

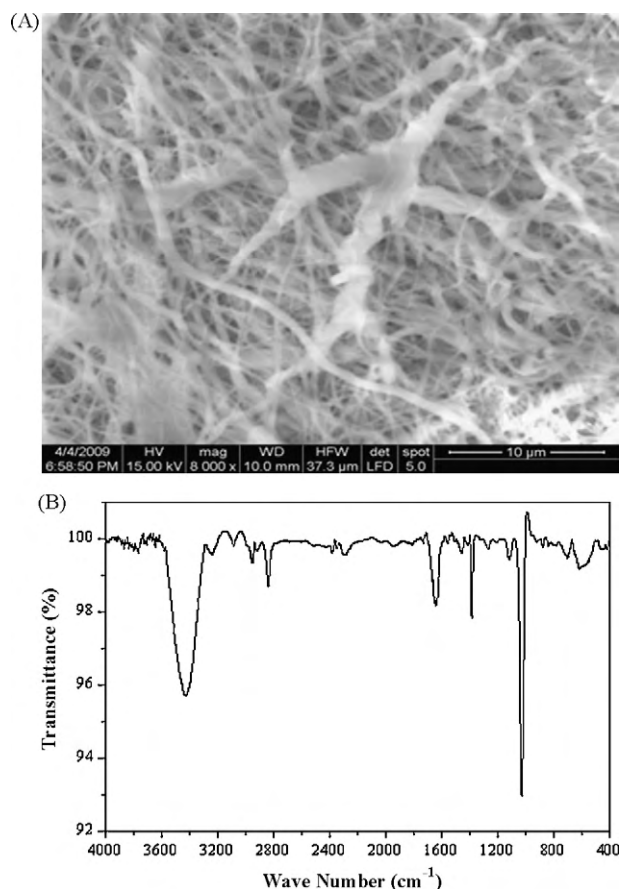
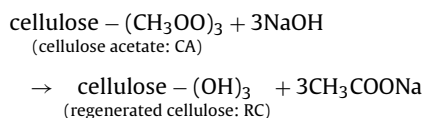


Fig. 7. (A) Scanning electron micrograph of a cellulose acetate nanofibrous membranes electrospun from a solution containing 12 wt% cellulose acetate, thermally treated at 208 °C for 1 h then alkali treated in 0.5 M NaOH solution for 24 h. (B) Infrared spectrum of a cellulose acetate nanofibrous membranes electrospun from a solution containing 12 wt% cellulose acetate, thermally treated at 208 °C for 1 h then alkali treated in 0.5 M NaOH solution for 24 h.

ize the remaining NaOH compared to the standard membrane-free titrations. This decrease is attributed to the consumption of variable amounts of NaOH for the removal of acetyl groups from the CA structure, and the consequent regeneration of cellulose. This takes place according to the following reaction:



The difference in the volumes consumed between the various types of membranes may be attributed to the original difference in their weights. It should be mentioned that the variation of the volumes of HCl needed for each type of CA was not pronounced after a maximum of 10 h treatment. This indicates a possible completion of the removal of acetyl groups after a maximum of 10 h only. Lu and Hsieh (2009) previously regenerated cellulose by treating CA membranes in 0.05 M aqueous NaOH solution for 24 h. Ma and Ramakrishna (2008) and Ma et al. (2005) carried out the same reaction for 24 h in a 0.1 M NaOH in an (ethanol:water of 2:1 by volume) or (ethanol:water of 4:1 by volume) solvent mixtures, respectively. Using higher concentration of NaOH in the current studies is thus considered the main cause of lowering the time needed for the deacetylation reaction to take place. To confirm the deacetylation of the nanofibrous membranes in the current study, they were investigated by IR spectroscopy as a function of alkali treatment time. A

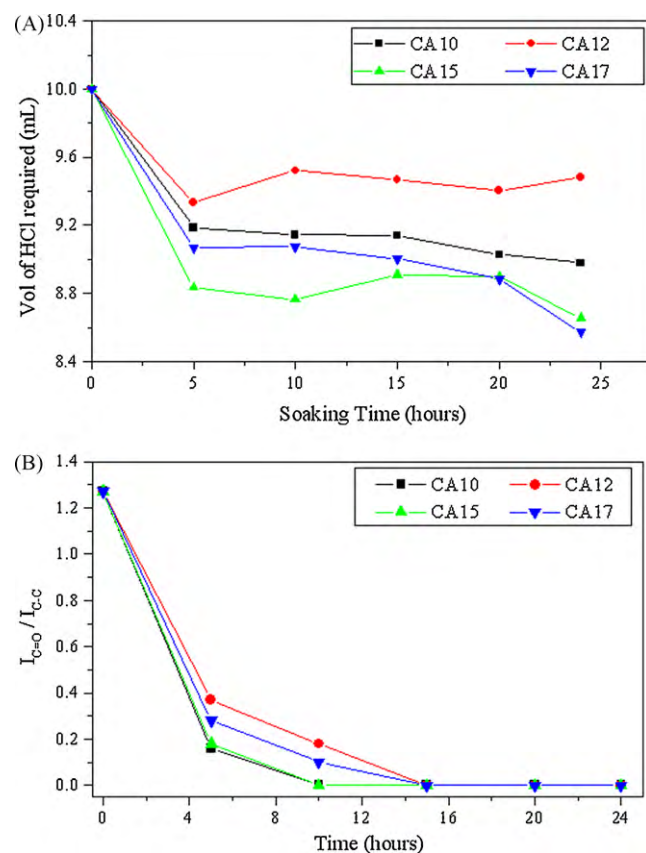


Fig. 8. (A) Volumes of HCl required to neutralize the un-reacted NaOH in each of the alkaline solutions after each time period of soaking the different cellulose acetate nanofibrous membranes. (B) Relative intensity of the C=O characteristic band at 1750 cm⁻¹ to the C–C characteristic band at 1375 cm⁻¹ as a function of soaking time (in h) during the alkaline treatment of CA10–17 nanofibrous membrane.

semi-quantitative analysis was carried out to follow-up the disappearance of the acetyl carbonyl group at 1750 cm⁻¹ with time, using a band at 1375 cm⁻¹, which is characteristic to the C–C absorption, as a reference band. Variation in the relative intensity of the carbonyl band to that of the C–C band ($I_{\text{C=O}}/I_{\text{C-C}}$) with time was followed. Results are shown in Fig. 8B, and revealed the complete disappearance of this band after a maximum of 10 h, and the consequent regeneration of cellulose. These findings, therefore, confirm the titration results previously shown in Fig. 8A.

The variation in the morphology of the membranes as a result of treating them in alkaline solutions is shown in Fig. 9. Unlike the conclusions drawn from Fig. 7, cellulose regeneration without a thermal pre-treatment seems not to affect the overall integrity of the fibers, where no distortion of the fibers was observed in all samples. However, comparing the fiber size distribution of these membranes, given in Fig. 9E, indicates a relative increase in the diameter of all fibers compared to the as spun and those thermally treated at 208 °C. This could be attributed to the swelling step that was carried out to increase the spacings between the fibers to facilitate the alkaline treatment reaction.

Thermal analysis of a representative regenerated cellulose membrane; RC12, was carried out by DSC. Compared with the DSC graphs in Fig. 3C, the DSC of the regenerated cellulose (RC12) showed an average T_g of 192.1 °C. The previous confirmation of the de-acetylation process by IR analysis excludes the possibility of presence of remaining CA in the tested membrane. Therefore, the presence of a T_g in the RC12 sample may be attributed to partial crystallization of the regenerated cellulose, although it was not easily identified by X-ray diffraction (Fig. 10).

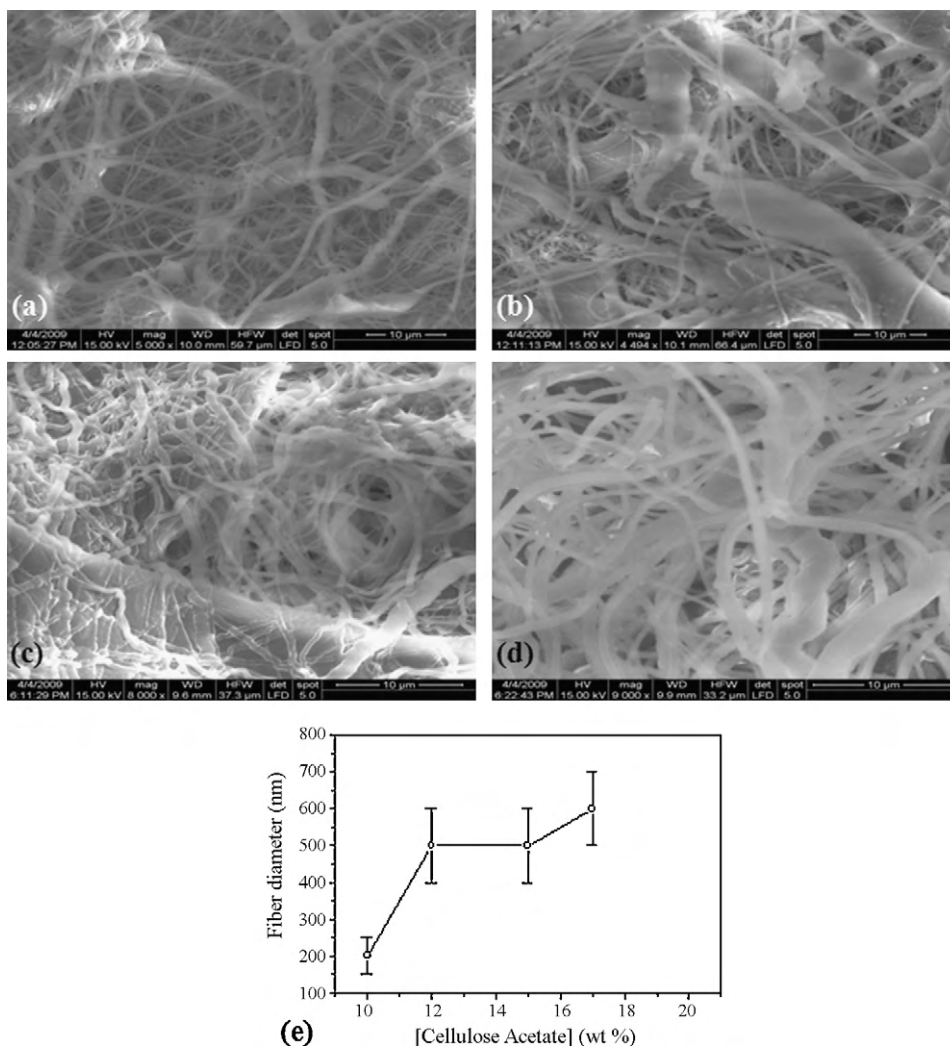


Fig. 9. Scanning electron micrographs of nanofibers electrospun from solutions containing (A) 10 wt%, (B) 12 wt%, (C) 15 wt%, and (D) 17 wt% cellulose acetate after thermal treatment in air at 208 °C for 1 h followed by soaking in 0.5 M NaOH solutions for 24 h, (E) average fiber size distribution as a function of distance.

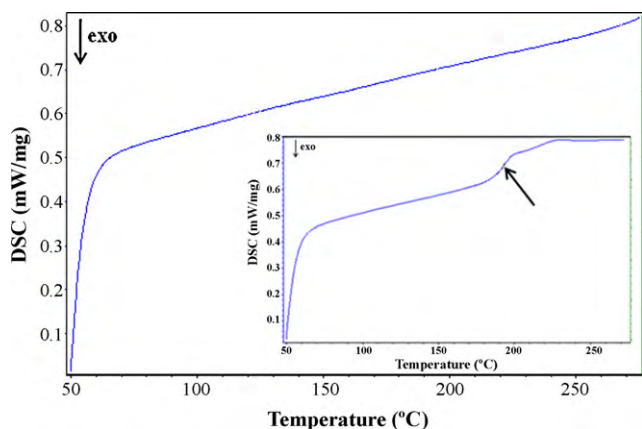


Fig. 10. Differential scanning calorimetric curve of a regenerated cellulose membrane made by alkaline treatment of a cellulose acetate nanofibrous membrane containing 12 wt% of cellulose acetate (insert shows details of the DSC graph with an arrow pointing to the T_g of the regenerated cellulose sample).

4. Summary

The current article investigated the effect of thermal and alkali treatment on the structural stability of cellulose nanofibrous

membranes made by an electrospinning technique. Nanofibrous membranes made from solutions containing 10–20 wt% of CA in acetone–DMAC solvent mixtures were investigated. Results showed the dependence of structural stability of the fibers on the procedure of thermal treatment, and the thickness of the membranes. An evidence of de-acetylation of the membranes as a result of thermal treatment was observed. Thermal treatment of thin CA sheets (<100 nm in thickness) followed by de-acetylation in alkaline solution showed damage of the nanofibers' morphology. De-acetylation of the as-spun nanofibrous membranes in alkaline solutions reached completion in less than 10 h without deteriorating the morphology of the nanofibers.

Acknowledgment

This work is part of the MSc thesis of Bothain Al Shamsi in the Environmental Science Program, UAE University.

References

- Al Shamsi, B. Polymeric Nanofibrous Media for Enhanced Ground Water Filtration, MSc. Thesis. UAE University, 2009.
- Barhate, R. S., & Ramakrishna, S. (2007). *Journal of Membrane Science*, 296, 1–8.
- Barud, H. S., Júnior, A. M., Santos, D. B., de Assunção, R. M., Meireles, C. S., Cerqueira, D. A., et al. (2008). *Thermochimica Acta*, 471, 61–69.
- Chen, L., Bromberg, L., Hatton, T. A., & Rutledge, G. C. (2008). *Polymer*, 49, 1266–1275.

- Frenot, A., Henriksson, M. W., & Walkenstrom, P. (2007). *Journal of Applied Polymer Science*, 103, 1473–1482.
- Frey, M. W. (2008). *Polymer Reviews*, 48, 378–391.
- Han, S., Son, W., Youk, J., Lee, T., & Park, W. H. (2005). *Materials Letters*, 59, 2998–3001.
- Han, S. O., Son, W. K., Youk, J. H., & Park, W. H. (2008). *Journal of Applied Polymer Science*, 107, 1954–1959.
- Han, S., Youk, J., Min, K., Kang, Y., & Park, W. (2008). *Materials Letters*, 62, 759–762.
- Kaur, S., Ma, Z., Chan, C., Ramakrishna, S., & Matsuura, T. (2006). *Journal of Membrane Science*, 281, 581–586.
- Kim, C., Frey, M. W., Marquez, M., & Joo, Y. L. (2005). *Journal of Polymer Science Part B: Polymer Physics*, 43, 1673–1683.
- Kim, C., Kim, D., Kang, S., Marquez, M., & Joo, Y. (2006). *Polymer*, 47, 5097–5107.
- Kim, J., Chen, Y., Kang, K., Park, Y., & Schwartz, M. (2008). *Journal of Applied Physics*, 104, 96104.
- Kulpinski, P. (2005). *Journal of Applied Polymer Science*, 98, 1473–1482.
- Liu, H., & Hsieh, Y. (2002). *Journal of Polymer Science Part B: Polymer Physics*, 40, 2119–2129.
- Liu, H., & Hsieh, Y. (2003). *Journal of Polymer Science Part B: Polymer Physics*, 41, 953–964.
- Lu, P., & Hsieh, Y. (2009). *Journal of Membrane Science*, 330, 288–296.
- Ma, Z., Kotaki, M., & Ramakrishna, S. (2005). *Journal of Membrane Science*, 265, 115–123.
- Ma, Z., & Ramakrishna, S. (2008). *Journal of Membrane Science*, 319, 23–28.
- Meier, M., Kanis, L., & Soldi, V. (2004). *International Journal of Pharmaceutics*, 278, 99–110.
- Park, J. Y., Han, S. W., & Lee, I. H. (2007). *Journal of Industrial and Engineering Chemistry*, 13, 1002–1008.
- Ritcharoen, W., Supphol, P., & Pavdsnt, P. (2008). *European Polymer Journal*, 44, 3963–3968.
- Son, W., Youk, J., Lee, T., & Park, W. (2004). *Journal of Polymer Science Part B: Polymer Physics*, 42, 5–11.
- Tang, C., & Liu, H. (2008). *Composites A*, 39, 1638–1643.
- Taylor, G. (1964). *Proceedings of the Royal Society of London Series A*, 280, 383.
- Tungprapa, S., Puangparn, T., Weerasombut, M., Jangchud, I., Fakum, P., Semongkhon, S., et al. (2007). *Cellulose*, 14, 563–575.
- Wang, M., Wang, L., & Huang, Y. (2007). *Journal of Applied Polymer Science*, 106, 2177–2184.
- Wu, X., Wang, L., Yu, H., & Huang, Y. (2005). *Journal of Applied Polymer Science*, 97, 1292–1297.
- Xu, S., Zhang, J., He, A., Li, J., Zhang, H., & Han, C. (2008). *Polymer*, 49, 2911–2917.
- Yoon, Y., Moon, H., Lyoo, W., Lee, T., & Park, W. (2009). *Carbohydrate Polymers*, 75, 246–250.
- Zeleny, J. (1914). *Physical Review*, 3, 69.
- Zhang, L., Menkhaus, T., & Fong, H. (2008). *Journal of Membrane Science*, 176–184.
- Zhao, S., Wu, X., Wang, L., & Huang, Y. (2003). *Cellulose*, 10, 405–409.
- Zhao, S., Wu, X., Wang, L., & Huang, Y. (2004). *Journal of Applied Polymer Science*, 91, 242–246.